Since January 2020 Elsevier has created a COVID-19 resource centre with free information in English and Mandarin on the novel coronavirus COVID-19. The COVID-19 resource centre is hosted on Elsevier Connect, the company's public news and information website.

Biosensors and Bioelectronics 70 (2015) 74–80

Contents lists available at ScienceDirect

Biosensors and Bioelectronics

journal homepage: www.elsevier.com/locate/bios

Impedimetric cell-based biosensor for real-time monitoring of cytopathic effects induced by dengue viruses

Ming Soon Cheng [a], Suk Hiang Lau [b], Kwai Peng Chan [c], Chee-Seng Toh [a], Vincent T. Chow [b,*]

[a] Division of Chemistry and Biological Chemistry, School of Physical and Mathematical Sciences, Nanyang Technological University, 21 Nanyang Link, Singapore 637371, Singapore
[b] Host and Pathogen Interactivity Laboratory, Department of Microbiology, Yong Loo Lin School of Medicine, 5 Science Drive 2, National University Health System, National University of Singapore, Singapore 117545, Singapore
[c] Virology Section, Department of Pathology, Singapore General Hospital, Outram Road, Singapore 169608, Singapore

ARTICLE INFO

Article history:
Received 10 December 2014
Received in revised form
8 March 2015
Accepted 9 March 2015
Available online 10 March 2015

Keywords:
Cytopathic effects
Dengue virus serotypes
Cell-based biosensor
Electrochemistry
Impedance
Poly-l-lysine
Screen-printed electrode

ABSTRACT

We describe an impedimetric cell-based biosensor constructed from poly-L-lysine (PLL)-modified screen-printed carbon electrode for real-time monitoring of dengue virus (DENV) infection of surface-immobilized baby hamster kidney (BHK-21) fibroblast cells. Cytopathic effects (CPE) induced by DENV-2 New Guinea C strain (including degenerative morphological changes, detachment, membrane degradation and death of host cells), were reflected by drastic decrease in impedance signal response detected as early as ~30 hours post-infection (hpi). In contrast, distinct CPE by conventional microscopy was evident only at ~72 hpi at the corresponding multiplicity of infection (MOI) of 10. A parameter that describes the kinetics of cytopathogenesis, CIT_{50}, which refers to the time taken for 50% reduction in impedance signal response, revealed an inverse linear relationship with virus titer and MOI. CIT_{50} values were also delayed by 31.5 h for each order of magnitude decrease in MOI. Therefore, based on the analysis of CIT_{50}, the virus titer of a given sample can be determined from the measured impedance signal response. Furthermore, consistent impedance results were also obtained with clinical isolates of the four DENV serotypes verified by RT-PCR and cycle sequencing. This impedimetric cell-based biosensor represents a label-free and continuous approach for the dynamic measurement of cellular responses toward DENV infection, and for detecting the presence of infectious viral particles.

1. Introduction

In recent decades, outbreaks of emerging and re-emerging diseases caused by infectious viruses such as dengue virus (DENV), ebola virus, influenza virus, severe acute respiratory syndrome coronavirus and West Nile virus pose ongoing threats to global biosecurity. In confronting these infectious diseases that spread well beyond the initial affected regions, their surveillance and control often create serious challenges for public health organizations. Hence, the development of rapid, effective and safe virus detection tools has become a major priority of the global community. Current clinical laboratory virus detection tests based on real-time and multiplex PCR techniques, provide a promising platform for simultaneous nucleic acid amplification and detection of multiple target sequences in a single test (Caliendo, 2011; Gullett and Nolte, 2015). However, these molecular techniques are incapable of identifying live infectious viral particles since they detect the nucleic acids originating from both infectious and non-infectious viruses. Virus samples usually comprise high viral particle-to-plaque-forming unit or PFU ratio (Cheng et al., 2012), which may indicate that the minority of viruses in a given sample is infectious, or the presence of non-infectious viruses with mutated or damaged genomes, or failure of most of the viruses to successfully infect due to the complexity of the infection cycle (van der Schaar et al., 2007). Proof of infectious viral particles is highly important and can only be accomplished by conventional cell culture assays, which is time-consuming and labor-intensive. Clearly, it is essential to develop an effective and simple virus detection tool for the assessment of virulence and identification of infectious viral particles to aid in the control of an epidemic.

The electrochemical impedance spectroscopic (EIS) technique has recently gained popularity in cell-based assays in view of advantages such as high sensitivity, non-invasive measurement, accessibility of time-dependent and quantitative data. Cell-based assays using adherent mammalian cell cultures such as fibroblast and endothelial cells have been utilized in toxicological and virological studies (Peters et al., 2012; Hofmann et al., 2013). Since the first reported application of EIS in cell culture study (Giaever

* Corresponding author. Fax: +65 67766872.
E-mail address: micctk@nus.edu.sg (V.T. Chow).

http://dx.doi.org/10.1016/j.bios.2015.03.018
0956-5663/

and Keese, 1984), this technique has been widely employed for in vitro monitoring of dynamic responses of cells toward drugs, toxic agents and pathogens (Kiilerich-Pedersen et al., 2011; Asphahani et al., 2012; Xu et al., 2012). Principally, the EIS cell-based analytical system involves quantitative monitoring of the spreading, morphology and viability of adhered cell cultures in real-time, by applying a constant alternating current (AC) electric field. Due to the low conductivity of cellular membrane, formation of a confluent cell monolayer on the electrode surface often constricts current flow. The corresponding change in impedance signal response can be continuously monitored to obtain information on cellular growth or coverage on the electrode surface (Cheung et al., 2005). Ultrasensitive impedimetric methods have recently reported non-invasive cell-based analyses of viral infections including herpes simplex virus infection of Vero cells (Cho et al., 2007), human cytomegalovirus infection of human fibroblasts (Kiilerich-Pedersen et al., 2011), and bluetongue virus infection of bovine endothelial cells (Drew et al., 2010). The direct, real-time investigation of DENV-induced cytopathogenesis in mammalian fibroblast cells using the EIS cell-based analytical system is first reported in this study.

Mosquito-borne dengue infections are caused by single-stranded RNA-containing DENV which is transmitted by *Aedes* mosquitoes. DENV exists as four antigenically distinct serotypes designated DENV-1, -2, -3 and -4 (Teles, 2011). Among the serotypes, secondary infection with DENV-2 has proven to be responsible for the more severe symptoms of dengue fever (Vaughn et al., 2000). Invasion of host cells by lytic viruses such as DENV will ultimately result in degenerative changes and damage to host cells, known as cytopathic or cytopathogenic effects (CPE). Such effects are generally characterized by degenerative morphological changes, detachment, membrane degradation and eventual death of cells. In general, decreased tight junctions between cells, and increased separation between cells and electrode arising from CPE may lead to decreased impedance signal response. In comparison to conventional inspection methods such as microscopy and plaque assay that rely on observable changes in the morphology and surface coverage of cells, the EIS technique offers a more promising platform for studying virus–host interactions based on the real-time measurement of CPE-induced impedance response (Cho et al., 2007).

Here we report an impedimetric cell-based biosensor constructed from poly-L-lysine (PLL)-modified screen-printed carbon electrode (SPCE) for real-time monitoring of DENV infection of surface-immobilized baby hamster kidney (BHK-21) fibroblast cells. This in vitro method in which the cell-based biosensor is immersed in the culture medium, detects viral-induced CPE by gradual decrease in the impedance response. The sensitivity of the biosensing system is enhanced using SPCE, which constricts the current to flow within a small area of working electrode (Campbell et al., 2007; Alonso-Lomillo et al., 2010). Furthermore, adherence of a cationic polymeric film (PLL) onto SPCE significantly improves the attachment and spreading of cells (Mazia et al., 1975; Sanders et al., 1975; Frey and Corn, 1996; Carrier and Pézolet, 1984; Khademhosseini et al., 2004; Sitterley, 2008). The excellent performance in terms of rapid detection time, automated analysis, high sensitivity and capability of indirectly identifying infectious viral particles are some desirable features of this impedimetric cell-based approach in real-time biosensing.

2. Materials and methods

2.1. Reagents and materials

SPCE, carbon working electrode, silver pseudo-reference electrode, and platinum auxiliary electrode on ceramic substrate were purchased from DropSens. PLL (MW 70,000–150,000 at 0.01% w/v) and potassium hexacyanoferrate (III) ($K_3Fe(CN)_6$, ~99%) were purchased from Sigma-Aldrich. Fetal bovine serum (FBS), and Dulbecco's phosphate-buffered saline (DPBS) without calcium and magnesium were obtained from Biowest. Trypsin–EDTA (10 ×) and penicillin–streptomycin (100 ×) were obtained from PAA Laboratories. RPMI-1640 medium was purchased from Thermo Scientific Hyclone. Avicel RC-591 (1.2% solid) was purchased from FMC BioPolymer.

2.2. Fabrication of PLL-modified SPCE

10 μL of 0.01% (w/v) sterile-filtered aqueous solution of PLL was applied onto the carbon electrode surface (with an area of 12.6 mm^2) and the tip of pipette was used to spread the solution evenly over the entire electrode surface. The electrode was inverted and placed in a drying oven at 80 °C for at least 5 min to ensure the transformation of PLL film into the stable β-sheet configuration, and adherence of PLL (at a thickness of 1.05 nm) to the electrode surface (Jordan et al., 1994). Excess PLL solution was aspirated, and the electrode surface was thoroughly rinsed with sterile ultrapure water. The PLL-modified SPCE was characterized using cyclic voltammetry (CV) in the presence of 1.0 mM $Fe(CN)_6^{3-/4-}$ in 1 × PBS, pH 7.4 at a scan rate of 100 mV s^{-1} and potential range from −0.8 to 0.8 V.

2.3. Culturing and maintenance of BHK-21 cells

BHK-21 cells (American Type Culture Collection) were cultured in a T25 tissue culture flask containing 3 mL of growth medium (RPMI-1640 medium supplemented with 10% FBS and 1 × penicillin–streptomycin solution). Cells were grown in a humidified incubator at 37 °C with 5% CO_2. When the cells were 80–90% confluent (after 1–2 days), growth medium was removed from the flask. Cells were washed once with 5 mL of 1 × DPBS, 3 mL of 1 × trypsin–EDTA was added, and incubated at 37 °C with 5% CO_2 for 5 min until cells detached. The detached cells were flushed, trypsin–EDTA was removed, the cells were subsequently resuspended in 2 mL of growth medium, and centrifuged at 6000 rpm for 1 min. The supernatant was discarded, and the cell pellet was resuspended in 3 mL of growth medium. BHK-21 cells were propagated at a sub-cultivation ratio of 1:2.

2.4. Preparation of DENV stocks

DENV-2 New Guinea C (NGC) strain and four clinical isolates each of DENV serotypes 1, 2, 3 and 4 were propagated in BHK-21 cells supplemented with maintenance medium (RPMI-1640 supplemented with 5% FBS, 1 × penicillin–streptomycin). Virus at multiplicity of infection (MOI) of 0.1 was inoculated, and the tissue culture infectious fluid (TCIF) was harvested 4–5 days upon the observation of CPE. MOI represents the ratio of the number of infectious agents (viruses) to the number of infection targets (cells) adsorbed on the electrode surface. Uninfected cells served as the control. TCIF was subsequently centrifuged at 6000 rpm for 1 min. The supernatant containing viruses was collected and diluted with RPMI-1640 to achieve the desired MOI for viral infection monitoring experiments. Plaque assay using Avicel (1.2%) and crystal violet staining was performed to determine the virus titer expressed as PFU mL^{-1}.

2.5. Construction of cell-based biosensor and monitoring of DENV-2 infection

The experimental set-up consists of a CHI 750D potentiostat-

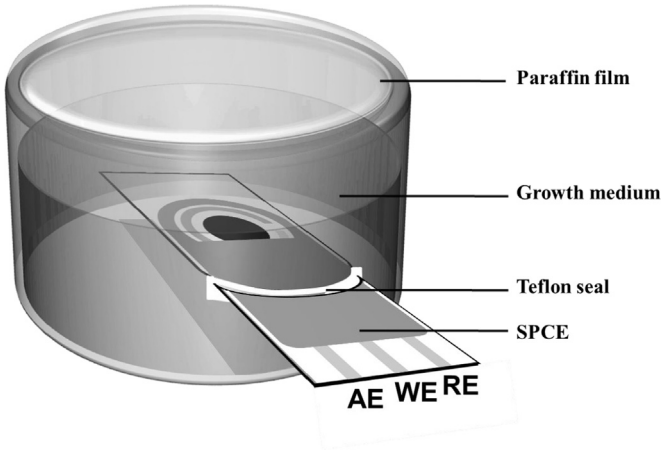

Fig. 1. Experimental set-up comprising a sterilized polypropylene vessel integrated with a poly-L-lysine (PLL)-modified screen-printed carbon electrode (SPCE), carbon working electrode (WE), silver pseudo-reference electrode (RE), and platinum auxiliary electrode (AE).

galvanostat (CH Instruments) with data acquisition software, and a sterilized polypropylene vessel integrated with a PLL-modified SPCE (Fig. 1). Total cell count was ascertained using TC10 Automated Cell Counter (Bio-Rad). Cell suspension with viable cell count of $>95\%$ was harvested to obtain a cell concentration of 5×10^5 cells mL^{-1}. BHK-21 cells (in 50 μL) were seeded on the PLL-coated carbon electrode surface, and allowed to attach and spread on the electrode surface for approximately 2 h. Thereafter, 10 mL of growth medium was gently added to the vessel. Cells were allowed to proliferate in an incubator at 37 °C with 5% CO_2 for 18 h. Subsequently, 500 μL of DENV-2 stock solution was added and mixed gently with cell medium. BHK-21 cells infected with DENV-2 at different MOI were incubated at 37 °C and 5% CO_2 for another 5 days. Proper sterilization of all apparatus and preparatory work were carried out in an antiseptic environment. The impedimetric properties of cell monolayers before and after viral infection were monitored at 37 °C using the EIS technique. Electrochemical impedance spectra were recorded at open circuit potential, frequency of 4 kHz, and excitation amplitude of 10 mV.

2.6. RNA isolation, reverse transcription (RT), polymerase chain reaction (PCR), and analysis of RT-PCR products of clinical isolates of dengue viruses

The Qiagen RNeasy Kit was employed to isolate total cytoplasmic RNA from TCIF collected from each DENV serotype (at MOI of 0.1) propagated in BHK-21 cells cultured with RPMI-1640 medium supplemented with 5% FBS, and incubated at 37 °C with 5% CO_2 for 5 days. Synthesis of cDNA (RT) was carried out using 200 ng of RNA, 200 U of Moloney Murine Leukemia Virus (M-MLV) reverse transcriptase (Promega), 10 U of RNase inhibitor, 2 mM of dNTPs, and 0.2 μM each of four downstream primers DSP 1, 2, 3, and 4, and subjected to 42 °C for 20 min. PCR was carried out using 100 ng of each cDNA and 0.2 μM each of primers, DSP 1, 2, 3, 4, and DV 1. The PCR cycles consisted of an initial denaturation at 95 °C for 5 min, followed by 35 cycles each of denaturation at 95 °C for 30 s, annealing at 50 °C for 30 s, extension at 72 °C for 30 s, and a final extension at 72 °C for 5 min (Seah et al., 1995a). PCR products (10 μl each) were electrophoresed for 1 h in 1% agarose gels (in 1 × TBE) containing SYBR Safe DNA gel stain (Life Technologies). Images were obtained using the ChemiDoc MP system (Bio-Rad). The specific PCR products corresponding to DENV serotypes 1, 2, 3, and 4 were excised and subjected to cycle DNA sequencing using BigDye Terminator Cycle Sequencing kit v3.1 and 3130xL Genetic Analyzer (Applied Biosystems).

3. Results and discussion

3.1. Cyclic voltammetric characterization of PLL-modified SPCE

Initially, we added cells to the bare SPCE and observed that the impedance signals were negligible and fluctuating between experiments compared with the baseline signals from the bare SPCE without cells added. The former signals remained unintelligible even when cells on the bare SPCE were infected with DENV (data not shown). These findings alluded to poor attachment of cells to the bare SPCE, which led us to modify the electrode by coating it with PLL to facilitate cell attachment.

The carbon working electrode surface of SPCE was modified with a cationic polymeric film (PLL) using a similar method described previously (Anson et al., 1983). The configuration of PLL in solution changes from random coil to α-helix at about pH 10. Subsequent heating to 80 °C promotes the transformation of the PLL film into the β-sheet configuration, which is believed to comprise chains that are partially cross-linked by hydrogen bonding. The cyclic voltammograms of the PLL-modified SPCE obtained in the presence of 1.0 mM $Fe(CN)_6^{3-/4-}$ in 1 × PBS, pH 7.4 (Fig. 2(A)) indicated fairly constant CV peak current responses for 100 repetitive potential cycles with RSD values of 5.71% and 2.90% for anodic and cathodic peak currents, respectively. This excellent stability of current response reflected strong adherence

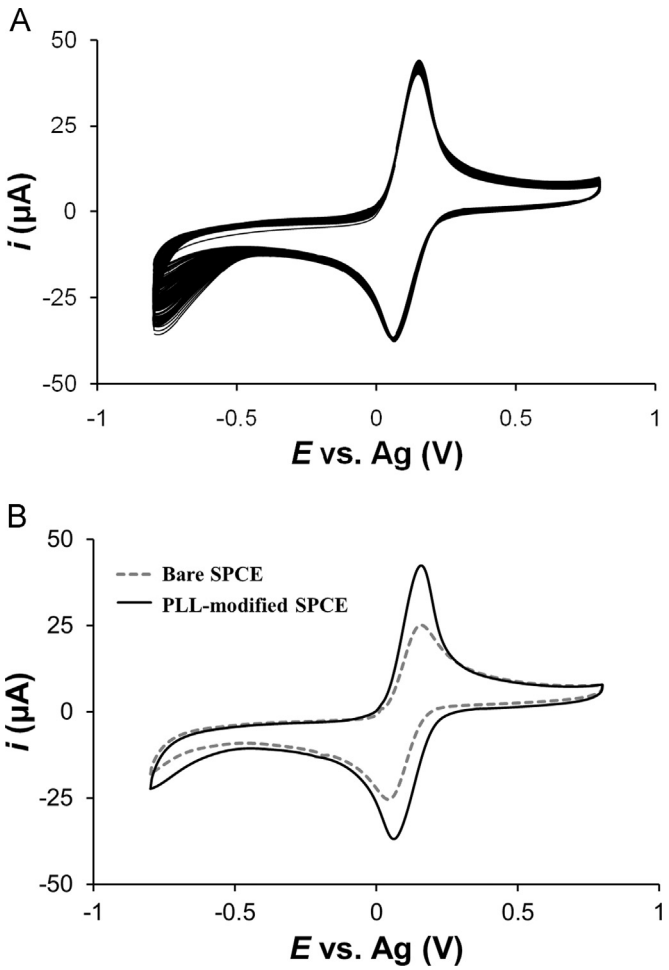

Fig. 2. (A) Repetitive potential cycling of a SPCE modified with 0.01% (w/v) PLL. (B) Comparison of the cyclic voltammetric current response between a bare SPCE (—) and a PLL-modified SPCE (— — —). Conditions: scan rate = 100 mV s^{-1}; potential range = −0.8 to 0.8 V; analysis solution containing 1.0 mM $Fe(CN)_6^{3-/4-}$ in 1 × PBS, pH 7.4.

of the PLL film to the carbon working electrode surface. In comparison to other electrode surfaces such as platinum and glassy carbon, PLL has been shown to be more resilient and strongly adhered onto the rough surface of screen-printed carbon (Fogg et al., 1995). The contrasting behavior of a bare SPCE and a SPCE modified with 0.01% (w/v) PLL toward the redox couple $Fe(CN)_6^{3-/4-}$ is shown in Fig. 2(B). The cyclic voltammograms of the PLL-modified SPCE exhibited a more reversible current response. Coating of electrode surface with a layer of cationic polymer PLL reduces the electrode overpotential and facilitates the redox reaction of anionic redox probes such as $Fe(CN)_6^{3-/4-}$ at the electrode surface. This enhanced anionic exchange capability of the cationic polymer-modified electrode is indicated by a 60.65% increase in CV peak current response compared to a bare electrode (Fig. 2(B)).

Electrode surface coating methods such as gelatin coating (Campbell et al., 2007) and equilibration with culture medium (McCoy and Wang, 2005; Muller et al., 2011) are commonly employed to promote the attachment and spreading of cells on the electrode surface. Despite their good biocompatibility, the utility of these methods is limited by the instability, weak adherence to the electrode surface, and poor cell capture capability. In this study, the positively charged PLL coating was adopted owing to its excellent cell capture capability and strong adherence to carbon electrode surface. Various studies have documented that adherent cell lines such as fibroblast and endothelial cells possess an overall negative surface charge, which facilitates their adhesion to positively charged surface (Somosy et al., 1986; Singh et al., 1992; Hamdan et al., 2006). This negative surface charge may be attributed to the carboxylic groups of aspartic and glutamic acid (p*Ka*=3.9–4.2) of proteins, carboxylic groups of sialic acid (p*Ka*=2.8) of glycoproteins, phosphate groups (p*Ka*=2.0), and sulfate groups (p*Ka*=1.9) of sulphated proteoglycans or glycoproteins (Singh et al., 1992). Another explanation is that their extracellular matrix is rich in negatively charged glucosaminoglycans (Somosy et al., 1986), thus suggesting that the observed cell adhesion behavior is mainly electrostatic in nature. The enhanced cationic properties of PLL-modified carbon electrode are therefore responsible for the strong adhesion of BHK-21 cells.

3.2. Real-time impedimetric monitoring of DENV infection

In this study, the virus–host interactions between DENV and BHK-21 cells were investigated by the EIS technique. BHK-21 cells constitute a type of adherent fibroblast cells, derived by single-cell isolation from the kidneys of five Syrian golden hamsters, *Mesocricetus auratus* (Stoker and Macpherson, 1964). This cell line is susceptible to infection by DENV, vesicular stomatitis virus, reovirus, and human adenovirus. The Bode diagram shown in Fig. 3(A) was generated from EIS spectra recorded at a frequency ranging from 100 Hz to 1 MHz. In the absence of electron mediator or redox probe, the electrode impedance of cells is limited by stray capacitance at high frequency and electrode polarization at low frequency. Moderate frequency (1–10 kHz) is well-suited for probing the cellular morphological changes induced by viral infection or cytotoxicants (McCoy and Wang, 2005; Campbell et al., 2007; Cho et al., 2007). The intermediate frequency at which the impedance signal was most affected by the change in cellular morphology was ~4 kHz (Fig. 3(A)), where the impedance signals measured between cells prior to virus inoculation and during day 5 of viral infection (at MOI=5) were considerably different from each other. Thus, the EIS data recorded at 4 kHz appear to provide meaningful results which may correlate with the morphological dynamics of cells and the kinetics of DENV-induced cytopathogenesis. This finding was further extended to the infection monitoring experiments where the impedance readings of cell adhesion and subsequent DENV infection were monitored at 4 kHz every 30 min up to 160 h.

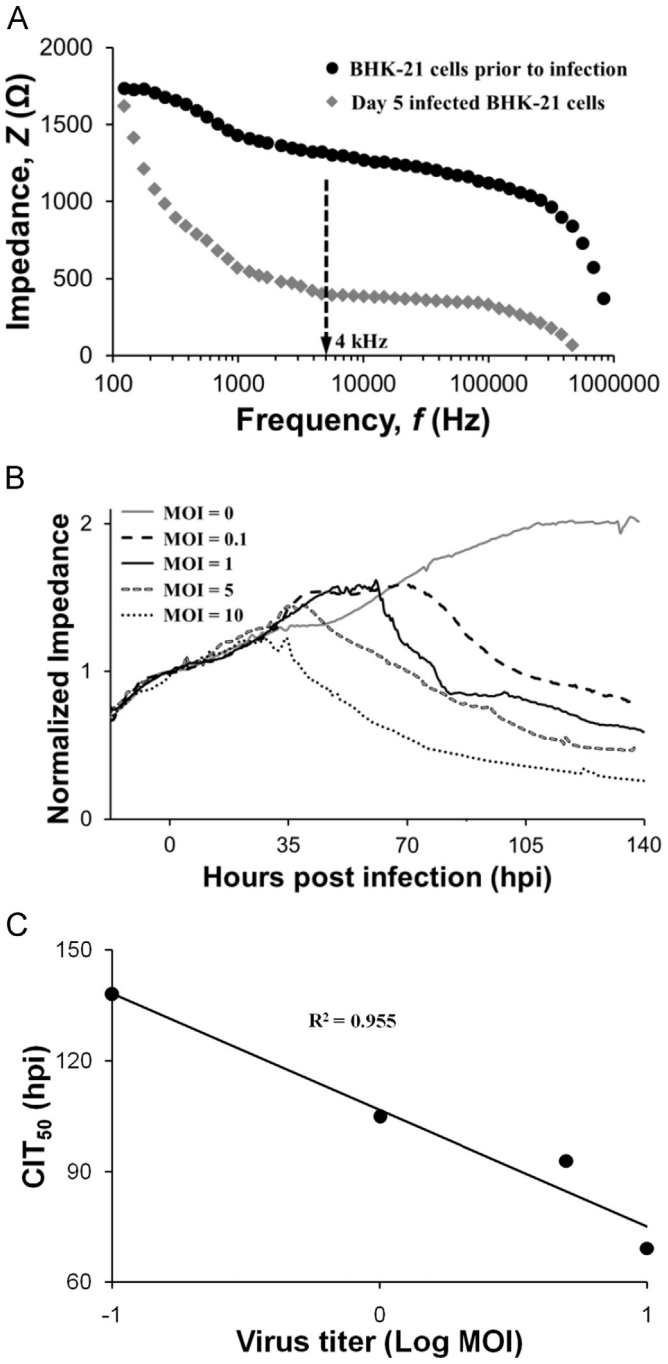

Fig. 3. (A) EIS Bode diagram recorded in a frequency range of 100 Hz to 1 MHz shows the impedance signal response of the BHK-21 cell-based biosensor measured prior to infection (●), and during day 5 of infection (♦) with DENV-2 (NGC strain) at MOI=5. (B) BHK-21 cell-based biosensor impedance signal as a function of DENV-2 NGC infection time at different MOI (0, 0.1, 1, 5, 10). Impedance signal response in the presence of virus (Z_{virus}) was normalized against the impedance signal response derived from the same biosensor in the absence of virus at 0 hpi ($Z_{virus}=0$). EIS data were recorded at open circuit potential, frequency of 4 kHz, and excitation amplitude of 10 mV. Vertical lines for each MOI indicate the onset of CPE. (C) Plot of CIT_{50} against the logarithm of virus titer (MOI). CIT_{50} refers to the time taken for 50% reduction in cell impedance.

Due to the variation of the coating of cells on the electrode surface, the impedance signals of four different cell-based biosensors at 25 hours post-infection (hpi) varied between 355.4 Ω and 508.5 Ω with a RSD of 16.5%. Normalization of the impedance

signal response in the presence of virus (Z_{virus}) against the response derived from the same biosensor in the absence of virus at 0 hpi ($Z_{virus}=0$) yielded a relatively low RSD of 4.6%. Normalization of the impedance signal against the blank signal enhances the reproducibility, precision of results, and avoids the need to calibrate each individual biosensor.

The DENV infection process involves several stages: attachment of viral envelope glycoprotein to cellular receptors such as dendritic cell-specific ICAM-3 grabbing nonintegrin (DC-SIGN), heparin sulfate or cell surface immunoglobulin (Chen et al., 1997; Tassaneetrithep et al., 2003). After fusion with the plasma membrane, viruses are enveloped in an acidified endocytic vesicle known as endosome, and subsequently release RNA into cytoplasm. Virus replication would eventually trigger membrane degradation and release viral progeny into the extracellular environment. In general, viral invasion of host cells induces a series of intra- and inter-cellular remodeling processes, which ultimately lead to changes in tight junctions between cells, and the distance between cells and electrode.

Fig. 3(B) shows the normalized impedance signal response as a function of viral infection time at different MOI. This plot reveals information on the attachment and growth of cells on the electrode surface, morphological dynamics of cells, and kinetics of viral-induced cytopathogenesis. Due to the low conductivity of cell membranes, the flow of moderate frequency current at the cell-electrode or cell-cell interface is sensitively influenced by nanometer changes in the adhesion regions or tight junctions between cells (Cheung et al., 2005). Thus, a gradual increase in the electrode impedance observed during cell culture indicates that cells are actively propagating and densely populating onto the PLL-modified carbon electrode surface. Impedance signal keeps on increasing after virus inoculation as cells continue to grow until cytopathogenesis induces a series of cellular remodeling processes that influence the morphology and adhesion of cells on the electrode surface. Viral-induced cytopathogenesis often results in severe morphological and physical changes, detachment of cells from surface, and eventual cell death (Campbell et al., 2007). In Fig. 3(B), fluctuation of the normalized impedance signal signifies the onset of CPE induced by DENV-2 NGC strain, followed by a drastic reduction in impedance signal response, which could be detected as early as ~30 hpi at MOI of 10. Moreover, after the observed CPE, the normalized impedance signal of the cell-based biosensor declined by 50% at ~69 hpi. Technically, this particular time taken for 50% reduction in the cell impedance response is termed $CIT_{50,}$ a kinetic parameter typically used to characterize the viral-induced cytopathic events (Fang et al., 2011). To further characterize the viral-induced cytopathogenesis, CIT_{50} was regressed as a function of virus titer in the logarithm of MOI. Fig. 3(C) displays an inverse linear relationship between virus titers and CIT_{50} values ($R^2=0.955$). The resultant regression indicates that CIT_{50} was delayed by 31.5 h for each order of magnitude decrease in MOI. Therefore, the dependence of the CPE-induced impedance signal response on the viral infectious dose permits the estimation of virus titers of viral samples based on the measured impedance signals.

3.3. Control and kinetics experiments

Several control experiments were carried out to assess the performance of impedimetric cell-based biosensor for the investigation of virus–host interactions. A control experiment using BHK-21 cells in the absence of DENV (represented by the black line in Fig. 3(B) produced a gradual increment in impedance signal with time. Clearly, BHK-21 cells cultured in growth medium remain viable and actively propagate on the electrode surface. The normalized impedance signal reaches its maximum after ~5 days

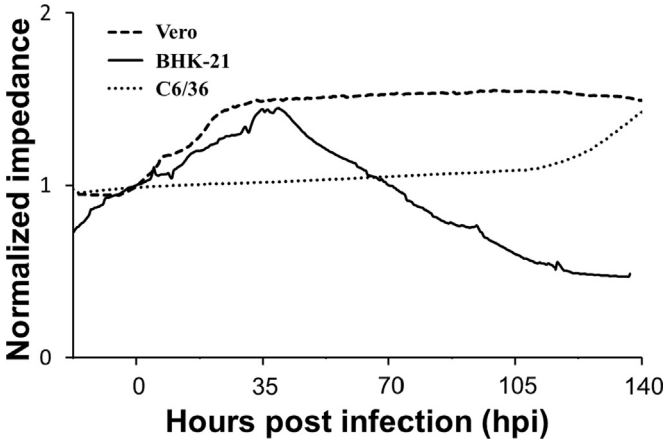

Fig. 4. Control experiments to compare biosensor impedance signal responses of Vero (– – –), BHK-21 (—), and C6/36 (●●●) cells toward DENV-2 NGC infection. EIS data were recorded at open circuit potential, frequency of 4 kHz, and excitation amplitude of 10 mV. Conditions: infection with DENV-2 (NGC strain); MOI=5; growth medium constitutes the background electrolyte.

of incubation with growth medium where the electrode surface is fully covered with cells. Another control experiment using a PLL-modified SPCE immersed in growth medium in the absence of BHK-21 cells and DENV gave a fairly constant impedance signal over a period of 6 days (data not shown). Fig. 4 shows the control experiments using different host cells infected with DENV-2 NGC strain at MOI of 5. In the control using biosensor prepared with Vero cells, a commonly used mammalian cell line, the electrode impedance increased initially as the Vero cells grew and reached a plateau from days 3 to 6. Another control using the C6/36 *Aedes albopictus* mosquito cell line produced a fairly constant impedance signal from days 0 to 5, thus revealing poor attachment and spreading of C6/36 cells on the PLL-modified carbon electrode surface. In summary, DENV-induced CPE could not be observed with Vero and C6/36 cell lines even at a relatively high MOI of 5. This suggests that the impedance response is specific to BHK-21 cells and may not relevant to other cell lines. In summary, decrease in impedance signal could only be detected with the occurrence of DENV-induced cytopathogenesis of the BHK-21 fibroblast cell line.

For comparison, DENV-2 NGC-infected BHK-21 cells seeded in a PLL-coated culture flask were observed for CPE using an EVOS FL digital fluorescence microscope (Life Technologies). Microscopic images were taken using a Sony high-sensitivity monochromatic CCD camera, with contrast and brightness adjusted to improve the quality of images. Uninfected BHK-21 cells served as control. Microscopic imaging of BHK-21 cells after 5 days of infection with DENV-2 NGC strain at MOI of 1 displayed typical CPE including considerable changes in cellular morphology. Detachment of cells from the surface was indicated by the presence of many empty spaces and rounded cells instead of the original completely confluent monolayer of spindle-shaped cells as depicted in Fig. 5(A). On the other hand, the monolayer of densely populated uninfected BHK-21 cells remained virtually intact after 5 days of incubation with growth medium (Fig. 5(B)).

To study the kinetics of CPE of BHK-21 cells infected with DENV-2 NGC at MOI of 1 and 10, monitoring by conventional microscopy was performed at 1, 6, 18, 24, 30, 42, 48, 54, 67, 72, 78, 90, 96, 102, 144 and 174 hpi. BHK-21 cells mock-infected with heat-inactivated DENV-2 NGC at "MOI" of 10, and BHK-21 cells treated with DENV-2 NGC viral RNA served as additional controls. As expected, no CPE was observed for both negative controls up to 174 hpi. However, the earliest distinct microscopic evidence of CPE was observed at 72 and 102 hpi for MOI of 10 and 1, respectively (Supp. Fig.).

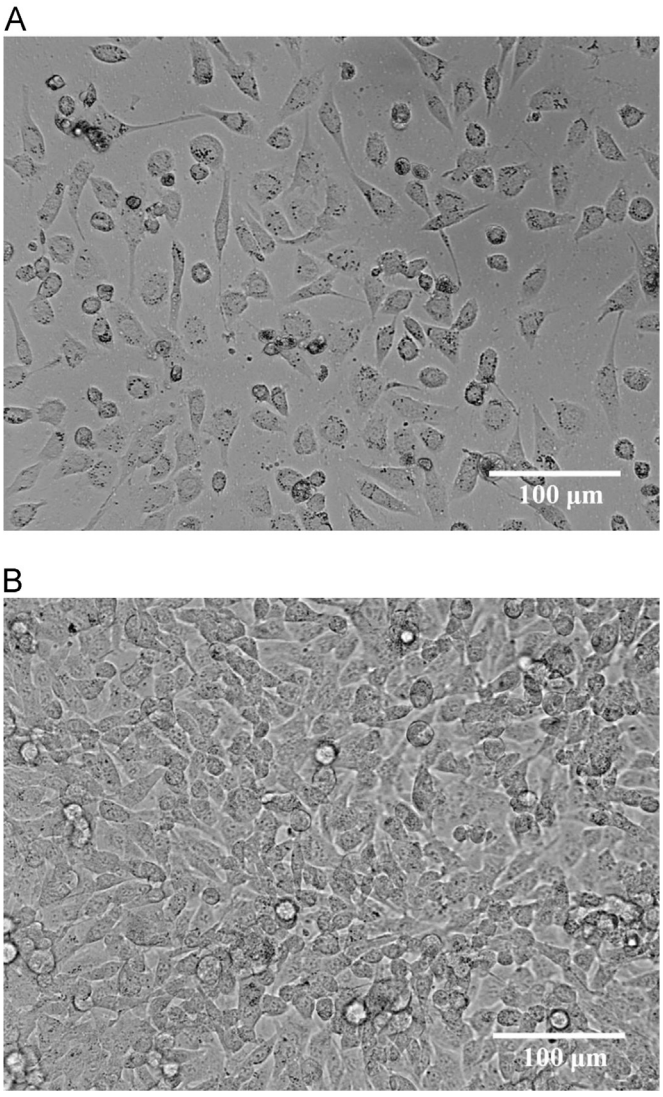

Fig. 5. Microscopic images of (A) BHK-21 cells after 5 days of infection with DENV-2 NGC at MOI = 1, and (B) control uninfected BHK-21 cells after 5 days of incubation with growth medium. Scale bar = 100 μm.

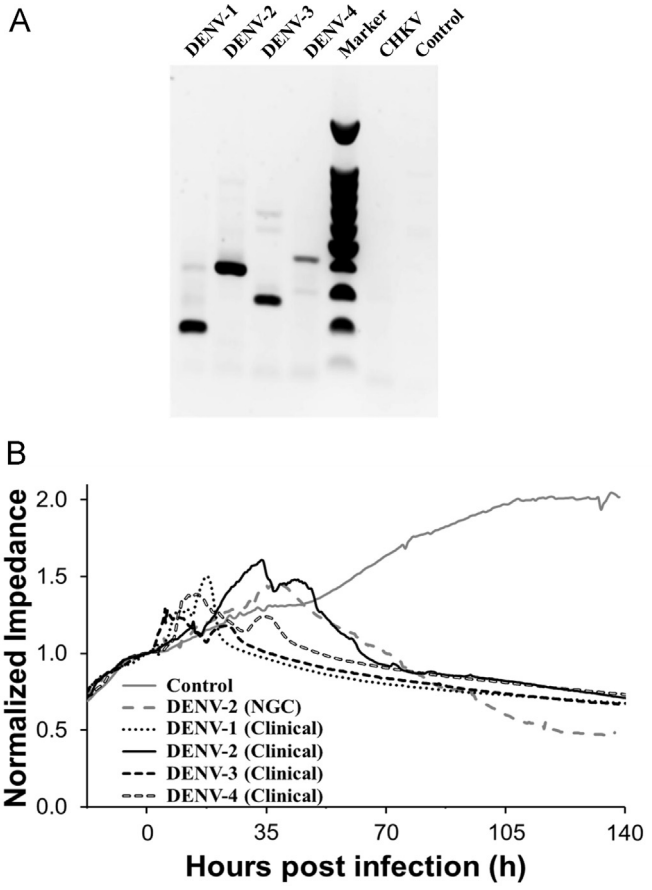

Fig. 6. (A) Specific typing of clinical DENV isolates by RT-PCR of cytoplasmic RNAs of virus-infected and uninfected BHK-21 cells. Agarose gel electrophoresis of RT-PCR products displaying diagnostic target sizes of 169, 362, 265 and 426 base-pairs (bp) for DENV-1, -2, -3 and -4, respectively, which were absent for Chikungunya virus-infected (CHKV) and uninfected BHK-21 cells (Control), thus showing good specificity. The 100-bp DNA ladder size marker was also included. (B) Normalized impedance signal response as a function of viral infection time for four different DENV serotypes isolated from clinical samples. DENV-2 NGC-infected cells and uninfected control cells were also included. EIS data were recorded at an open circuit potential, frequency of 4 kHz, and excitation amplitude of 10 mV. Vertical lines for each virus indicate the onset of CPE. Conditions: MOI = 5, BHK-21 host cells; growth medium constitutes the background electrolyte.

In direct comparison to the optical method, the more sensitive cell biosensor could "sense" CPE much earlier as reflected by the drastic reduction in impedance signal response at ~30 and ~60 hpi for MOI of 10 and 1, respectively.

3.4. Analysis of clinical DENV isolates

The potential application of cell-based biosensor in analyzing clinical isolates was examined against four different dengue serotypes, DENV-1, -2, -3, and -4. These viruses were isolated from the respective DENV-infected patients. The four clinical DENV isolates were verified to be DENV-1, -2, -3, and -4 strains by RT-PCR and cycle sequencing of amplified products (Seah et al., 1995a), and their sequences deposited in the GenBank database under accession numbers KM586232, KM979356, KP119840. Fig. 6 (A) shows agarose gel electrophoresis of the RT-PCR products of DENV-1, -2, -3, and -4. Their nucleotide sequences exhibit high identities to isolates RR121 (92%), 1046DN/1976 (97%), TB16 (97%), and 475A (99%), respectively. Infection of BHK-21 cells with the four clinical isolates of DENV was monitored by using the procedures described for the NGC strain. Fig. 6(B) displays similar CPE-induced impedance signals for the four clinical isolates (at MOI of 5). Slight variation in CPE detection time may possibly be attributed to the varying degrees of CPE induced by these clinical DENV strains. In summary, CPE induced by the four clinical isolates of DENV could be detected within 1–2 days post-infection. The performance of this impedimetric cell-based biosensor underscores its utility for the analysis of clinical DENV isolates. Future studies are warranted to evaluate this biosensor for the analysis of actual clinical specimens from dengue patients, e.g. blood samples (Seah et al., 1995b; Phanthanawiboon et al., 2014).

4. Conclusions

In conclusion, an impedimetric cell-based biosensor constructed from PLL-modified SPCE has proven to be useful for real-time monitoring of DENV-induced cytopathogenesis on surface-immobilized fibroblast cells. Based on this platform, CPE reflected by the drastic decrease in impedance signal response could be detected at ~30 hpi at MOI of 10. This impedimetric biosensing system outperforms conventional microscopic inspection that requires 3–5 days of DENV infection to conclusively observe the changes in morphology and surface coverage of cells. Other

attractive features of this cell-based biosensor include the possibility of automation, non-invasive measurement, reduced timeframe for the diagnosis of live DENV infection, mediatorless and label-free monitoring procedure, and capability of detecting the presence of infectious dengue viral particles to complement existing diagnostic tests such as RT-PCR and serology. In addition, virus titers of given viral samples can be estimated from the measured impedance signals by analysis of CIT_{50} values. The utility of this impedimetric cell-based biosensor for detecting clinical infectious viral isolates also demonstrates its potential application in the clinical setting.

Acknowledgements

The authors thank the Singapore Immunology Network, Agency for Science, Technology and Research for research grant funding. CMS acknowledges Nanyang Technological University for supporting his Ph.D. scholarship. We thank Dr. Justin Chu for providing Chikungunya virus as control.

Appendix A. Supplementary material

Supplementary data associated with this article can be found in the online version at http://dx.doi.org/10.1016/j.bios.2015.03.018.

References

Alonso-Lomillo, M.A., Dominguez-Renedo, O., Arcos-Martinez, M.J., 2010. Talanta 82, 1629–1636.
Anson, F.C., Saveant, J.M., Shigehara, K., 1983. J. Am. Chem. Soc. 105, 1096–1106.
Asphahani, F., Thein, M., Wang, K., Wood, D., Wong, S.S., Xu, J., Zhang, M.Q., 2012. Analyst 137, 3011–3019.
Caliendo, A.M., 2011. Clin. Infect. Dis. 52, S326–S330.
Campbell, C.E., Laane, M.M., Haugarvoll, E., Giaever, I., 2007. Biosens. Bioelectron. 23, 536–542.
Carrier, D., Pézolet, M., 1984. Biophys. J. 46, 497–506.
Chen, Y.P., Maguire, T., Hileman, R.E., Fromm, J.R., Esko, J.D., Linhardt, R.J., Marks, R.M., 1997. Nat. Med. 3, 866–871.
Cheng, M.S., Ho, J.S., Tan, C.H., Wong, J.P.S., Ng, L.C., Toh, C.S., 2012. Anal. Chim. Acta 725, 74–80.
Cheung, K., Gawad, S., Renaud, P., 2005. Cytom. Part A 65A, 124–132.
Cho, S., Becker, S., von Briesen, H., Thielecke, H., 2007. Sens. Actuator B – Chem. 123, 978–982.
Drew, C.P., Gardner, I.A., Mayo, C.E., Matsuo, E., Roy, P., MacLachlan, N.J., 2010. Vet. Immunol. Immunopathol. 136, 108–115.
Fang, Y., Ye, P.F., Wang, X.B., Xu, X., Reisen, W., 2011. J. Virol. Methods 173, 251–258.
Fogg, A.G., Pirzad, R., Moreira, J.C., Davies, A.E., 1995. Anal. Proc. 32, 209–212.
Frey, B.L., Corn, R.M., 1996. Anal. Chem. 68, 3187–3193.
Giaever, I., Keese, C.R., 1984. Proc. Natl. Acad. Sci. USA 81, 3761–3764.
Gullett, J.C., Nolte, F.S., 2015. Clin. Chem. 61, 72–78.
Hamdan, M., Blanco, L., Khraisat, A., Tresguerres, I.F., 2006. Clin. Implant Dent. Relat. Res. 8, 32–38.
Hofmann, U., Michaelis, S., Winckler, T., Wegener, J., Feller, K.H., 2013. Biosens. Bioelectron. 39, 156–162.
Jordan, C.E., Frey, B.L., Kornguth, S., Corn, R.M., 1994. Langmuir 10, 3642–3648.
Khademhosseini, A., Suh, K.Y., Yang, J.M., Eng, G., Yeh, J., Levenberg, S., Langer, R., 2004. Biomaterials 25, 3583–3592.
Kiilerich-Pedersen, K., Poulsen, C.R., Jain, T., Rozlosnik, N., 2011. Biosens. Bioelectron. 28, 386–392.
Mazia, D., Schatten, G., Sale, W., 1975. J. Cell Biol. 66, 198–200.
McCoy, M.H., Wang, E., 2005. J. Virol. Methods 130, 157–161.
Muller, J., Thirion, C., Pfaffl, M.W., 2011. Biosens. Bioelectron. 26, 2000–2005.
Peters, M.F., Scott, C.W., Ochalski, R., Dragan, Y.P., 2012. Assay Drug Dev. Technol. 10, 525–532.
Phanthanawiboon, S., A-nuegoonpipat, A., Panngarm, N., Limkittikul, K., Ikuta, K., Anantapreecha, S., Kurosu, T.J., 2014. Virol. Methods 209, 55–61.
Sanders, S.K., Alexander, E.L., Braylan, R.C., 1975. J. Cell Biol. 67, 476–480.
Seah, C.L., Chow, V.T., Tan, H.C., Chan, Y.C., 1995a. J. Virol. Methods 51, 193–200.
Seah, C.L., Chow, V.T., Chan, Y.C., Doraisingham, S., 1995b. Serodiagn. Immunother. Infect. Dis. 7, 55–58.
Singh, A.K., Kasinath, B.S., Lewis, E.J., 1992. Biochim. Biophys. Acta 1120, 337–342.
Sitterley, G., 2008. Bio Files 3, 8–9.
Somosy, Z., Kubasova, T., Ecsedi, G.S., Koteles, G.J., 1986. Int. J. Radiat. Biol. 49, 969–978.
Stoker, M., Macpherson, I., 1964. Nature 203, 1355–1357.
Tassaneetrithep, B., Burgess, T.H., Granelli-Piperno, A., Trumpfherer, C., Finke, J., Sun, W., Eller, M.A., Pattanapanyasat, K., Sarasombath, S., Birx, D.L., Steinman, R.M., Schlesinger, S., Marovich, M.A., 2003. J. Exp. Med. 197, 823–829.
Teles, F., 2011. Anal. Chim. Acta 687, 28–42.
van der Schaar, H.M., Rust, M.J., Waarts, B.L., van der Ende-Metselaarl, H., Kuhn, R.J., Wilschut, J., Zhuang, X.W., Smit, J.M., 2007. J. Virol. 81, 12019–12028.
Vaughn, D.W., Green, S., Kalayanarooj, S., Innis, B.L., Nimmannitya, S., Suntayakorn, S., Endy, T.P., Raengsakulrach, B., Rothman, A.L., Ennis, F.A., Nisalak, A., 2000. J. Infect. Dis. 181, 2–9.
Xu, Y.C., Lv, Y., Wang, L., Xing, W.L., Cheng, J., 2012. Biosens. Bioelectron. 32, 300–304.